Russian Chemical Reviews **71** (12) 981 – 991 (2002) © 2002 Russian Academy of Sciences and Turpion Ltd

DOI 10.1070/RC2002v071n12ABEH000751

Metal-oxide based nanoobjects: reactivity, building blocks for polymeric structures and structural variety †

A Müller, S Roy

Contents

I.	Introduction	981
II.	Reactions at well-defined sites of well-defined nanoobjects: an example	981
III.	Nanoobjects as building blocks for extended structures	982
IV.	Extending the structural variety	986
V.	Conclusion	990

Abstract. From the unique 'library' of molybdenum-oxide based building blocks/fragments under reducing conditions in aqueous solution a huge variety of nanoobjects, allowing specific reactions at well-defined positions, can be generated. This enables us to perform a new type of nanochemistry. Examples include the well-known molecular big-wheel of the type {Mo$_{176}$} and big-ball of the type {Mo$_{132}$} including their derivatives which are considered here. In addition, the by far largest structurally well-characterised cluster having 368 molybdenum atoms with the shape of a lemon is outlined and discussed. The bibliography includes 71 references.

I. Introduction

The deliberate synthesis of multifunctional compounds and materials from well-known building blocks which can be easily generated or are available from a 'virtual' library is one of the most challenging problems in contemporary chemistry. Pertinent targets include the synthesis of materials, *e.g.*, based on cross-linked building blocks with desirable electronic properties. In solutions of oxoanions of the early transition elements an enormous variety of compounds can be formed by linking together metal – oxygen building blocks.[1–9] The corresponding reactions are based on libraries with (virtual) building blocks, *i.e.* polyoxometallate (POM) fragments which, under appropriate conditions, lead to the generation of clusters ranging from those of mere aesthetic beauty to unusual materials. Examples include the spherical cluster anion $\{Mo^{VI}_{72}Mo^{V}_{60}O_{372}(CH_3COO)_{30}(H_2O)_{72}\}^{42-}$ (also known as an inorganic superfullerene or keplerate‡), and the ring-shaped cluster anion $\{Mo^{VI}_{126}Mo^{V}_{28}O_{462}H_{14}(H_2O)_{70}\}^{14-}$ (see Fig. 1 and reviews cited above). Additionally, interesting molecular magnets, novel-type supramolecular compounds, compounds with extended structures including those with mesoporous networks,[3–7] and surfactant-encapsulated giant clusters soluble in organic solvents (with the option of generating monolayers and Langmuir – Blodgett films) can be obtained.[10–14] In this context, we intend here to demonstrate perspectives for a new type of nanochemistry by highlighting:

— the possibility of performing reactions at well-defined positions of well-defined nanoobjects;

— the possibility of linking the nanoobjects;

— the possibility of obtaining numerous novel giant members of this 'nanosociety'.

The results described here are not included in previous reviews.[1–9]

II. Reactions at well-defined sites of well-defined nanoobjects: an example

1. Synthetic and structural aspects

The possibility of performing chemical reactions at well-defined sites of well-defined nanoobjects opens up interesting perspectives for the chemist, especially if novel functionalities emerge.[1–17] For example, the high-yield facile synthesis of giant spherical {Mo$_{132}$} (Fig. 1 *a*)[18] and ring-shaped {Mo$_{154}$} (Fig. 1 *b*)[19,20] (first reported in Ref. 19 but not with optimal synthesis) molybdenum-oxide based clusters provides us with easily accessible nanostructured landscapes with nano-sized cavities and a variety of different functional groups. In particular, it proved possible to incorporate paramagnetic metal centres, *e.g.*, Cu^{2+} ions, inside the tetrahedral cavities of the {Mo$_{154}$}-type rings formed by four O atoms with appropriate size. It is significant that our approach paves the way to the deliberate synthesis of a broad range of compounds, which can be obtained by altering the boundary conditions, such as the pH, temperature, and/or the presence of different substrates, while on the other hand, it also opens up new perspectives for studies in the sense of a novel type of self-assembly (see also Ref. 21).

The synthesis of a cluster containing Cu^{2+} ions involves reduction of an acidified aqueous polymolybdate with copper powder. The ammonium salt of this cluster is obtained as the black crystalline compound **1**.[15]

$$(NH_4)_{26}[(H_4Cu^{II}_5)Mo^{V}_{28}Mo^{VI}_{114}O_{432}(H_2O)_{58}]\cdot ca.\ 300\,H_2O$$

1

Single crystal X-ray diffraction studies show the presence of the $[\{Mo^{V/VI}_8O_{26}(\mu_3\text{-}O)_2X_i(H_2O)_3Mo^{V/VI}\}_{14}\{Mo^{VI}_2O_5(H_2O)_2\}_8]^{26-}$ cluster anion (ΣX_i = 4H + 5Cu) (**1a**), which can be considered as

A Müller, S Roy Inorganic Chemistry I, Department of Chemistry, Bielefeld University, PO Box 100131, D-33501 Bielefeld, Germany. Fax: (49-521) 106 60 03. E-mail: a.mueller@uni-bielefeld.de (A Müller), soumyajit.roy@uni-bielefeld.de (S Roy)

Received 12 July 2002
Uspekhi Khimii **71** (12) 1107 – 1119 (2002)
The English text provided by the authors

† Dedicated to Prof. Ilya Moiseev.

‡ By definition, keplerates are compounds having one central point, the barycentre (either occupied by an atom or vacant), around which one or more spherical shells of atoms contained in the cluster are located. These atoms are vertices of Platonic or Archimedean solids.

a derivative of the aforementioned prototypal tetradecameric ring-shaped cluster anion $\{Mo_{154}\}$, ($\{Mo_{154}\} \equiv \{Mo_8\}_{14}\{Mo_1\}_{14}\{Mo_2\}_{14}$) (**2a**).[4–7] The cluster anion **1a** lacks six $\{Mo_2\}$ building blocks as compared to the parent $\{Mo_{154}\}$ anion. Moreover, it contains non-uniformly distributed Cu^{2+} centres — with a maximal occupation number of 0.73 — in the 14 tetrahedral cavities marked by four oxygen atoms. The Cu^{2+} cations replace five of the 14 protons of the parent cluster **2a**, which are bonded to one of the two μ_3-O atoms that are involved in the formation of the cavities (Fig. 2). In the case of high H^+ ion concentrations, the maximum degree of protonation is attained, *i.e.*, all fourteen cavities of the cluster **1a** are occupied by protons bonded to the μ_3-O bridging atom.[5] In presence of the $HCOONH_4$ buffer, the degree of protonation of cluster **1a** is lower and consequently Cu^{2+} ions can be coordinated to the basic four O atoms of the corresponding tetrahedral cavity.

2. Electronic spectra and magnetic aspects

Although the resonance Raman (λ_e = 1064 nm) and IR spectra of **1a** are nearly identical to those of the parent cluster **2a**, the electronic spectrum of the former exhibits, as a result of the abundance of Cu^{2+} centres, an additional band at ~520 nm and a blue shift of the higher energy intervalence charge transfer (IVCT) transition localised in the $\{Mo_5^{V/VI}O_6\}$-type compartments,[5] each of them containing two delocalised 4*d* electrons. The change in the charge transfer is caused by the fact that the encapsulated Cu^{2+} ions are coordinated to the μ_3-O atoms which belong to the $\{Mo_5O_6\}$ compartments, thus resulting in an electron density redistribution in this compartment.

The room-temperature EPR powder spectrum of compound **1** is similar to the spectra of tetrahedral copper complexes containing $\{CuX_4\}$ groups, in particular, $\{CuO_4\}$ types, and therefore indicating the presence of Cu^{2+} (d^9) centres. The spectrum is characterised by g_x = 2.07, g_y = 2.15, and g_z = 2.37, as well as by the hyperfine splitting constant A_z = 125 G (related to the nuclear spin of $^{63/65}$Cu with I = 3/2). The values indicate that the $Cu^{2+}\cdots Cu^{2+}$ magnetic interactions are practically negligible ($Cu\cdots Cu \approx 6.2$ Å). This observation is also supported by magnetic susceptibility measurements. At high temperatures, the $\chi_{mol}T$ curve was found to reach a plateau at ~2.86 emu K mol^{-1}, which corresponds to about six Cu^{2+} centres per formula unit for g = 2.2. As the calculated inter- and intramolecular antiferromagnetic coupling constants are very small, $\chi_{mol}T$ decreases only at temperatures below ~20 K. The temperature variation of the magnetic susceptibility can be described using the Curie–Weiss equation

$$\chi = \frac{c}{T-\theta}$$

with a very low Weiss temperature (θ = −0.5 K).[15]

3. General aspects

Modification of the parent $\{Mo_{154}\}$ ring-type cluster anion **2a** — by introduction of paramagnetic Cu^{2+} ions under certain self-assembly conditions — is possible because of the presence of O_4-type cavities with dimensions in agreement with the characteristic Cu–O distances (2.0 ± 0.1 Å). The assembly of this cluster starts from simple mononuclear $\{MO_n\}$-type units, followed by the construction of larger intermediate building blocks (abundant in a virtual 'library'), which are finally transformed into a mesoscopic organised complex ring-shaped structure — with a variety of functional groups — *via* molecular recognition processes for Cu^{2+} centres which get integrated at the suitable sites of the cluster.

The highly symmetrical mesoscopic $\{Mo_{154}\}$-type parent cluster (see Fig. 1), which is the primary target of the self-assembly process in this case based only on molybdate, can undergo a variety of modifications due to alteration of the boundary conditions, or in other words, due to environmental influences, as for example, the presence of Cu^{2+} ions.

In this context, it is important to remember that assembly processes based on simple building blocks lead preferably to highly symmetrical species,§ such as rings.[4,5] This is consistent with many observations in cluster chemistry (see, for example, Ref. 24). Important is in this context that mesoscopic systems can, in spite of a high overall symmetry, exhibit versatile reactivity owing to the presence of large numbers of substructures with different functional groups. This feature is especially noteworthy as the accepted view is that higher symmetry leads to a decrease in the number of structural details and therefore reactivities. This rule actually only holds for smaller discrete species and crystalline systems with macroscopic homogenicity and microscopic translational invariance but not for discrete mesoscopic molecular-type species. An example for relevant mesoscopic systems is the situation with spherical viruses, mentioned in most biochemistry books.

It follows from the foregoing discussion that the molybdenum-oxide based ring-shaped clusters can be considered as nanostructured landscapes having a variety of functional groups at well-defined positions.[4–7,20] This permits various types of reactions, including catalytic ones, to be carried out at strictly defined positions. These reactions include coordination of activated ligands, but also amphiphilic and multiphilic ones (for example, diprotonated cysteine ligands ¶), which may lead to the generation of unusual surfaces within the cavities,[25] and the incorporation of metal centres or small fragments into appropriate cavities.

Another conclusion related to this work is that the reactivity and the electron density distribution in nanoobjects can be varied both by defect generations and by incorporation of open-shell heterometal atoms. In this particular case, the influence of the Cu^{2+} metal centres on the distribution of delocalised electrons within the above-mentioned compartments is indicated by the shift of the IVCT band from ~750 nm for the parent $\{Mo_{154}\}$ anion [5] to ~680 nm for anion **1a**.[15] Thus, one can adjust (tune) the electron density distribution, and even the related catalytic activity of the present type of nanoobjects, which can act as selective oxidants.[26]

III. Nanoobjects as building blocks for extended structures

1. Synthetic and structural aspects

The search for extended structures based on linked nano-sized stable (!) building blocks and possessing specified electronic and magnetic properties is an exceptionally worthy task because such compounds could provide new types of functionalised materials.[27] In this context we attempted the synthesis of the large well-defined metal-oxide based nanoparticles with unique host properties in order to use them as building blocks. Linking these blocks according to M–O–M or M–O–M' patterns can furnish, in principle, a broad range of compounds differing in architecture.

Our route to unique extended structures involved the use of spherical metal-oxide based keplerate-type clusters with icosahedral symmetry.[4,5] (The internal cavity diameter in this type of structures is sufficiently large even for encapsulating Keggin-type clusters. The related composites could be prepared through a facile synthesis.[28]) Linking such large spherical objects gives rise

§ The process can formally (!) be correlated with a general symmetry formalism or symmetry-evolution principle for a quasi-isolated system.[22] One important aspect of the symmetry-evolution principle is that the highly symmetrical species are often also preferably formed as they are kinetically inert. However, this principle is inapplicable to macroscopic chemical reaction systems as structure-formation-based precipitation is equivalent to symmetry breaking.[23]

¶ Multiphilic ligands like cysteine containing various functional groups ($-NH_3^+$, $-CO_2H$, $-S-S-$) can be coordinated to the inert wall of the cavity.

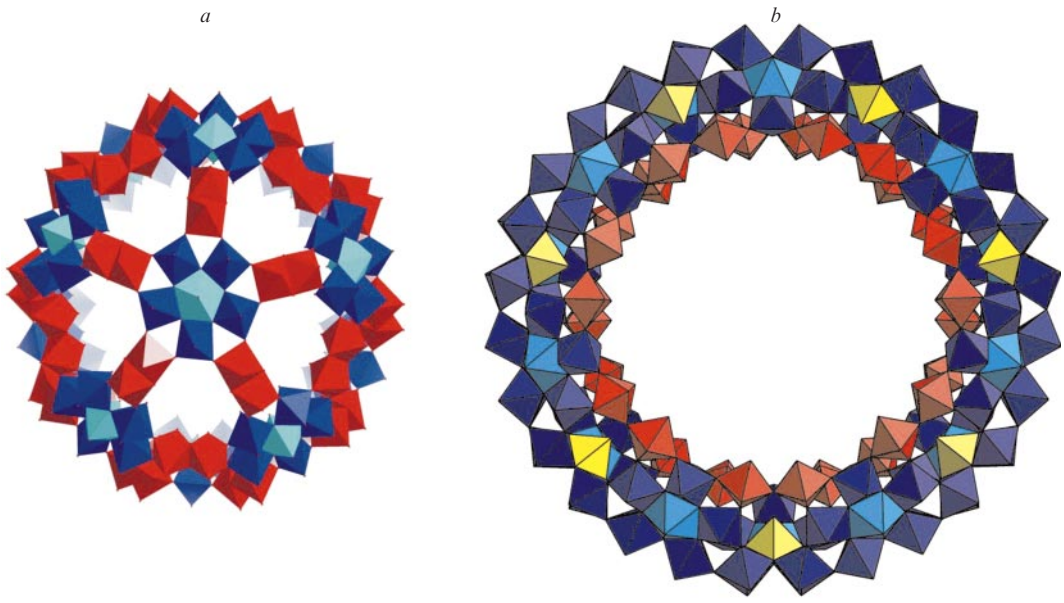


Figure 1. Spherical $\{Mo_{132}\}$- (*a*) and ring-shaped $\{Mo_{154}\}$-type (*b*) clusters (the $\{Mo_1\}$ unit cannot be seen in this view; see Fig. 2) shown in polyhedral representation. The spherical cluster shows the pentagonal units in blue and the linkers in red.

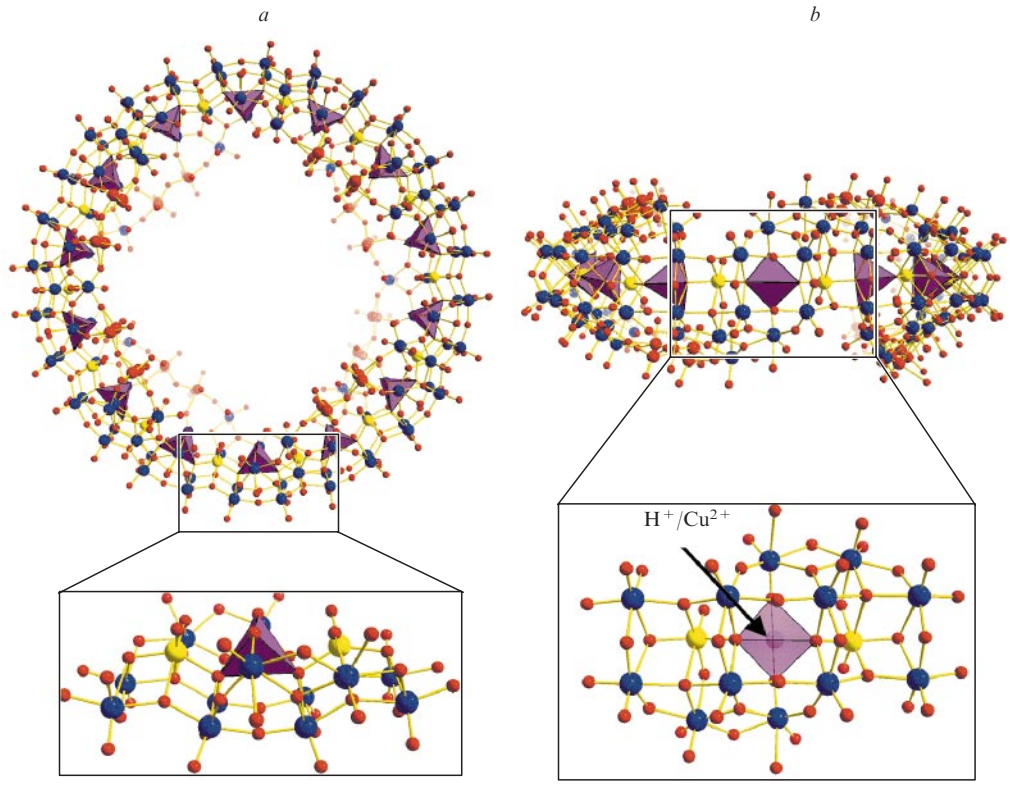


Figure 2. Molecular structure of the cluster anion **1a** [top (*a*) and side (*b*) views] in crystals of **1** in the atomic representation. The $\{O_4(Cu)\}$ tetrahedra are given in polyhedral representation. Colour code: oxygen is red, molybdenum is blue, except those of the $\{Mo_1\}$ shown in yellow. This drawing was first published in Ref. 15.

for instance to chain-type structures. Analogous chain structures are also produced upon linking fullerenes.[29–31]

As an example, we shall consider the synthesis and structure of an unusual mixed-valence compound **3**, containing the discrete $\{Mo^{VI}(Mo^{VI})_5\}_{12}\{Mo^{V}_6Fe^{III}_{24}\}$-type keplerate cluster **3a**.[16]

$$Na_2[\{Mo^{VI}(Mo^{VI})_5\}_{12}\{Mo^{V}_6Fe^{III}_{24}\}(CH_3COO)_{20}O_{258}(H_2O)_{84}]\cdot ca.\ 150\,H_2O$$

3

The black compound **3** is formed upon the addition of iron(II) chloride to an aqueous solution of sodium molybdate acidified with acetic acid in presence of air. Upon drying, a novel type of room-temperature solid-state reaction takes place, yielding compound **4** with a chain structure.[16]

$$\{Na_2[\{Mo^{VI}(Mo^{VI})_5\}_{12}\{Mo^{V}_6Fe^{III}_{24}\}(CH_3COO)_{20}O_{258}(H_2O)_{82}]\cdot ca.\ 80\,H_2O\}_n$$

4

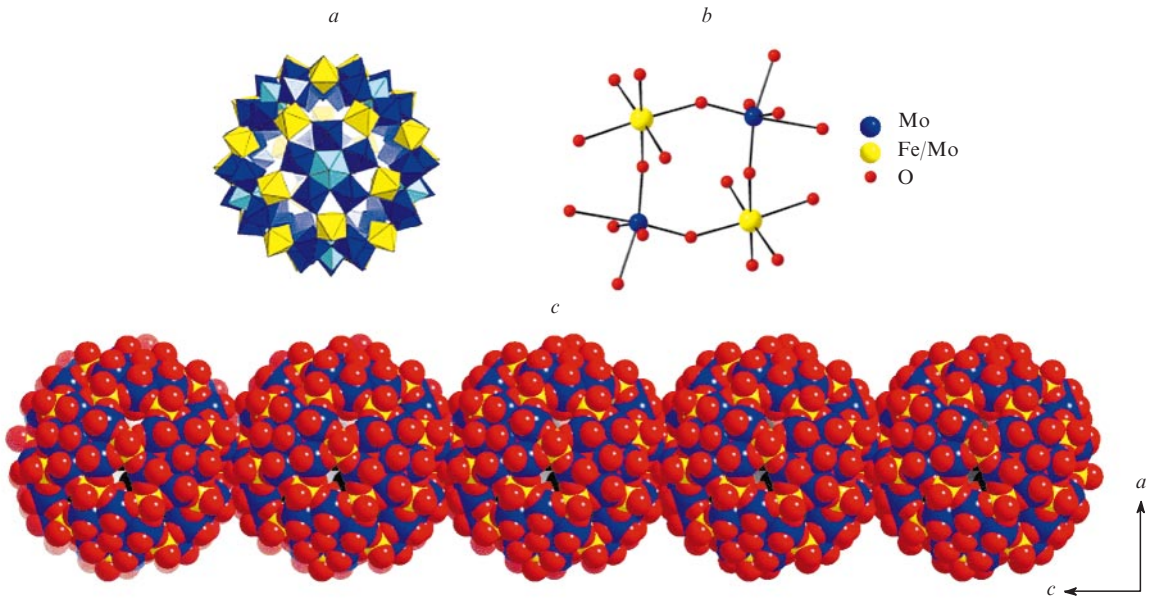


Figure 3. Structure of the discrete anion **3a** in crystals of **3** (*a*, polyhedral representation); structure of the chain **4a** in crystals of **4** (*c*, space-filling representation; the Mo positions can be identified), and the linking area of the chain **4a** [*b*, atomic representation; bond lengths (Å) and angles (deg) in the $\{M_4O_4\}$ rings (M = Mo/Fe): Mo–O: 1.72–1.78; Fe–O: 1.96–1.98; Mo–O–Fe: 147.0–149.9; O–Mo–O: 101.5; O–Fe–O: 93.2]. This drawing was first published in Ref. 16.

(In general, mixed-valence compounds of this type with extended structures possess remarkable electronic properties.[32])

During the formation of **3**, Fe^{II} ions are oxidised to Fe^{III}, only a minor portion of the Fe^{II} ions being used to reduce Mo^{VI} centres. Nevertheless, the presence of Fe^{II} ions is necessary, because beginning the synthesis with Fe^{III} as the starting material leads even in the presence of a reducing agent immediately to a non-crystalline precipitate.

Both the spherical cluster $[\{Mo^{VI}(Mo^{VI})_5\}_{12}\{Mo^{V}_6Fe^{III}_{24}\}.(CH_3COO)_{20}O_{258}(H_2O)_{84}]^{2-}$ (**3a**) (note: there is an error limit in the charge) and the related chains comprise 12 pentagonal $\{Mo^{VI}(Mo^{VI}_5O_{21})\}$-type building blocks, containing a central pentagonal $\{MoO_7\}$ bipyramid sharing edges with five $\{MoO_6\}$ octahedra. The pentagonal fragments are connected through 24 $\{Fe^{III}(H_2O)_2\}^{3+}$ and 6 $\{Mo^{V}O(H_2O)\}^{3+}$ linkers which are statistically distributed over the 30 vertices of an icosidodecahedron.† The six 4*d* electrons of the Mo linkers are partially delocalised over positions of the pentagonal $\{Mo(Mo_5)\}$ building groups. The bidentate acetate ligands are located inside the sphere and are coordinated simultaneously to the two metal atoms Fe and Mo. Thus, they function as bridges between the Fe and Mo centres. In the crystals of **4**, the icosahedral spherical building blocks, *i.e.*, of the type $\{Mo(Mo)_5\}_{12}\{Mo_6Fe_{24}\}$ (Fig. 3*a*), are linked to form chains (Figs 3 and 4 as well as Scheme 1) through Mo_A-O-Fe_B and a Fe_A-O-Mo_B group (A and B stand for two neighbouring spheres). This results in a nearly square $\{Fe_2Mo_2\}$ fragment (Fig. 3*b*) the centre of which coincides with a crystallographic inversion centre. Interestingly, the geometric details of the Fe_A-O-Mo_A- (inside a sphere), Fe_A-O-Mo_B- and Fe_B-O-Mo_A-type units do not differ significantly (Mo···Fe ~3.6 Å). As shown below, this has important implications for the magnetic properties of compound **4**. The $\{Fe_2Mo_2\}$ square fragment in **4** is topologically equivalent to the cyclobutane fragment found in dumbbell-shaped $\{C_{60}\}_2$ dimers. The latter unit is also built up by two intra- and two inter-sphere C–C bonds.[29]

† The presence of octahedral $Fe^{III}O_6$ groups could also be proved by Mössbauer spectroscopy. The presence of one $\{Mo^{VI}O\}^{4+}$ linker group, instead of $\{Mo^{V}O\}^{3+}$, and the related change of the number of Na atoms cannot be completely ruled out within the error limits of the invoked analytical techniques.

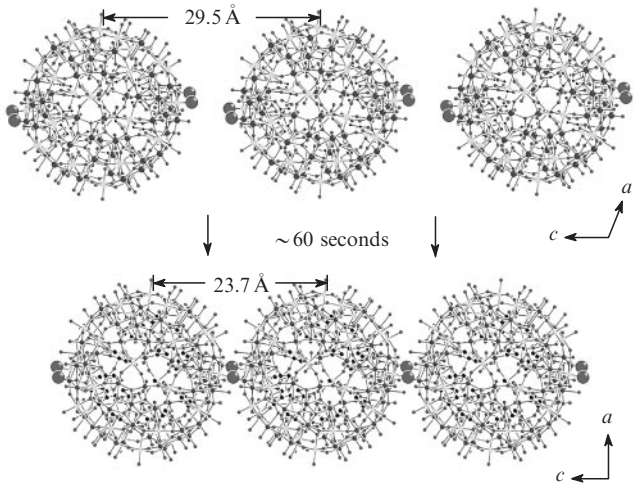
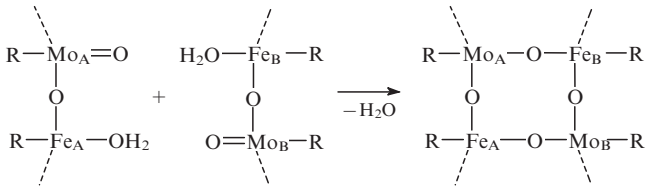


Figure 4. Schematic demonstration of the room-temperature solid-state reaction leading to the formation of the chain of **4** caused by linking the spheres **3a**. This drawing was first published in Ref. 16.

When compound **3** loses crystal water, the discrete spherical clusters **3a** approach one another, which is followed by their condensation to give infinite chains. The linking is caused by the fact that H_2O ligands in the $\{Fe^{III}(H_2O)_2\}^{3+}$ fragments in sphere A are substituted by terminal Mo=O groups of the $\{Mo(Mo_5)\}$ pentagons belonging to the neighbouring sphere B. Thus, the Mo=O group formally acts as ligand in accordance with the following Scheme 1.

Scheme 1



R = H_2O or CH_3COO.

The reaction is driven by the gain in entropy caused by the release of water molecules. This solid-phase S_N-type reaction, which functions well for compound **3**, does not happen, however, for the yellow compound **5**

$$[Mo_{72}Fe_{30}O_{252}(CH_3COO)_{12}\{Mo_2O_7(H_2O)\}_2\{H_2Mo_2O_8(H_2O)\}(H_2O)_{91}]\cdot \cdot ca.\,150\,H_2O\,,$$

5

which contains the $\{Mo^{VI}(Mo^{VI}_5)\}_{12}\{Fe^{III}_{30}\}$-type discrete neutral clusters.[33, 34] The reason is that cluster **3** shows the S_N-type reaction initiated by the Mo=O groups due to the increase in the electron density on the terminal oxygen atoms of these groups caused by the influence of six partially delocalised 4*d* electrons, which are not abundant in the non-reduced **5**.

Not only the crystallinity but also the space group ($P2_1/n$) is preserved throughout the solid-state reaction **3** → **4**. Comparison of the packing of the spherical clusters **3a** in the crystal lattices of compounds **3** and **4** has shown that the distances between the spherical $\{Mo(Mo)_5\}_{12}\{Mo_6Fe_{24}\}$-type units in **4** are shortened drastically along the crystallographic *c* axis (see Fig. 4) compared to the corresponding distances in **3**; as a result, the crystal lattice parameter *c* in **4** is 5.7 Å shorter than that in **3**.

2. An interesting mesoscopic magnetism

A convenient way of explaining the magnetism of compound **4** is to compare it with the cluster of compound **5** (see Refs 33, 34), which is the largest molecular paramagnet known.[35] In both systems, the antiferromagnetic exchange interactions between the Fe(III) centres ($S = 5/2$) abundant in a nearly perfect octahedral environment are mediated by the O−Mo−O groups.

In the case of **5**, the $\chi_{mol}T$ value increases with an increase in *T* from 20 to 300 K (Fig. 5), and at room temperature, it approaches the value expected for 30 uncorrelated centres with $S = 5/2$, namely, 131.25 emu K mol^{-1} (the spin-only value for $g = 2.0$). The room-temperature value of $\chi_{mol}T$ found for compound **4** is equal to 104.0 emu K mol^{-1}, which is closely similar to the value (105.0 emu K mol^{-1}) expected for 24 uncorrelated Fe(III) centres with $S = 5/2$. Since the partially delocalised Mo 4*d* electrons in **4**, as in the reduced $\{Mo_{102}\}$-type keplerate,[36] are strongly coupled, they contribute only to a negligible extent to the overall magnetic moment. Thus, the high-temperature results indicate that six of the thirty positions of the icosidodecahedron occupied by Fe(III) magnetic centres in the cluster of **5** are occupied in **4** by effectively non-magnetic centres. The magnetic susceptibilities measured in the 20−300 K range are in very good agreement with the Curie−Weiss function down to very low temperatures; however, the Weiss temperatures calculated for **4** and **5** differ significantly: $\theta(\mathbf{4}) = -13$ K, $\theta(\mathbf{5}) = -21.6$ K.

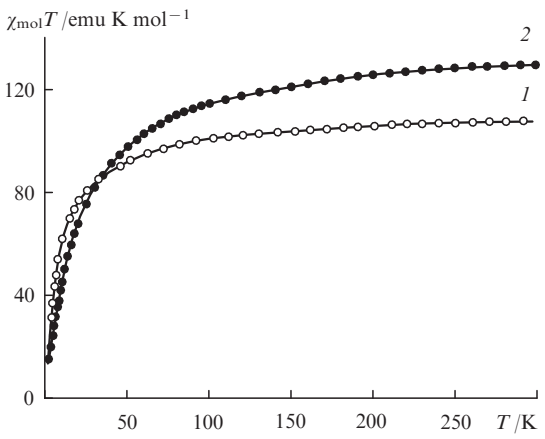


Figure 5. Comparison of the temperature dependences of $\chi_{mol}T$ for compounds **4** (curve *1*) and **5** (curve *2*).

These θ(**4**) and θ(**5**) values can be explained in terms of the following simple model. Since the geometric parameters of the corresponding Fe−O−Mo−O−Fe groups, including the bridges between the spheres, are virtually identical in compounds **4** and **5**, the same single Heisenberg exchange constant *J* is assumed for the nearest-neighbour Fe···Fe interactions (see Ref. 37). Important is that θ is proportional to the absolute number of nearest-neighbour Fe···Fe contacts per sphere.‡ This number is lower for compound **4** than for **5**, due to the presence of six centres that do not effectively contribute to paramagnetism, *i.e.*, that are effectively non-magnetic. A uniform statistical distribution of the non-magnetic centres over the 30 icosidodecahedron vertices results in 38 Fe···Fe contacts compared to the 62 contacts of a hypothetical all-iron configuration including 60 icosidodecahedron edges and 2 distinct bridges to the adjoining spheres in the chain. Thus, proceeding from the value $\theta(\mathbf{5}) = -21.6$ K, we obtain $\theta(\mathbf{4}) = 38/62 \times \theta(\mathbf{5}) = -13.2$ K, which is in excellent agreement with the value experimentally determined.

It is of interest to compare the case of uniform distribution of effectively non-magnetic centres with other distribution patterns, for example, the arrangement of all the non-magnetic centres on neighbouring sites of the icosidodecahedron. In this case, the Weiss temperature should increase to −18 K. Thus, the calculated θ(**4**) value perfectly reflects the uniform distribution of the magnetic centres in each individual sphere (with a ratio of the numbers of magnetic to non-magnetic positions equal to 24 : 6). If the average ratio equal to 24 : 6 is retained, while the magnetic to non-magnetic centre ratio in different spheres can be different, this situation cannot strictly correspond to the determined Curie–Weiss parameter. It is noteworthy that, because the Weiss temperature reflects the ordering and the distribution of the non-magnetic centres over the thirty possible positions, this value can be used to draw structural conclusions that cannot be obtained from the single crystal X-ray structure analysis.§

3. General outlook

Now we consider an interesting result related to the chemistry of extended structures. Spherical molybdenum-oxide based keplerate-type clusters possess a number of interesting features,[28] in particular, they can be used as building blocks in the development of various extended structures and nanomaterials. The linking of nano-sized spherical capsule-type objects, for instance, can lead to one-dimensional chains *via* a room-temperature solid-state reaction which can be regarded as a type of crystal engineering process. In view of the fact that we are dealing with spherical capsules of the type (Pentagon)$_{12}$(Linker)$_{30}$ (Linker = $\{Fe(H_2O)\}^{3+}$, see Refs 33, 34, $\{MoO(H_2O)\}^{3+}$, see Ref. 36), the linkers L can be changed stepwise with the option to change the surface properties. For example, by changing appropriately the degree of electron density on the surface of cluster **3**, by increasing in the present case the number of $\{MoO(H_2O)\}^{3+}$ groups, the nucleophilicity of this cluster can correspondingly be increased, which could lead to different types of inter-sphere condensation reactions. In summary, the type of linking of the spherical units depends on the MoO^{3+}/Fe^{III} ratio.

In addition, the presence of two $Fe^{II}\cdots Mo^{VI}$ and $Fe^{III}\cdots Mo^{V}$ couples with very close redox potentials makes compounds **3** and **4** especially interesting. In particular, this type of electronic structure can induce a temperature-dependent electron transfer in **4a**. In this context it is important to realize that the Fe and Mo atoms

‡ This result follows from the standard expression for θ determined for systems with a single exchange constant.

§ Single-crystal X-ray structure analysis does not allow one to distinguish between the situation of all spherical units having the same composition (as in the present case) and the situation where certain spheres have different compositions but also yield altogether for the whole compound the same Fe^{III}/Mo^{V} average ratio of 24 : 6.

in solid metal oxides which occupy octahedral positions obey the following equilibrium:[38]

$$Mo^{VI} + Fe^{II} \rightleftharpoons Fe^{III} + Mo^{V}.$$

The mentioned type of electron transfer is similar to electron delocalisation or hopping in 'heteropoly blues'.[1] This was confirmed by quantum-chemical calculations for electron transfer transitions in substituted (at the metal) polyoxometallates and by Mössbauer spectroscopy data for the iron-substituted cerium salt of 12-molybdenophosphoric acid, containing 0.6 Fe^{II} atoms as the counter-cations and 0.9 Fe^{II} atoms in the Keggin part.[39] The Mössbauer spectrum of this compound measured at room temperature differed from the spectrum recorded at very low (4.2 K) temperature.[39] Other examples of electron hopping and delocalisation in mixed-valence oxometallate clusters have also been reported.[40]

Finally, the **3** → **4** transformation and the resulting products are just one of a myriad of options that can be achieved in the future investigations of 'our' POM system.

IV. Extending the structural variety

1. General aspects

Nature's evolution from the primordial earth to the present overwhelming variety of macroscopic forms and functionalities, the formation of which is directed by their molecular 'counterparts', *i.e.*, nano-sized biomolecules, should stimulate thoughts about the potential of material systems in general and the related first principles, *i.e.* natural laws.

We refer to processes based on reservoir systems containing appropriate building blocks, the linking of which can lead to an overwhelming or even, in a kind of combinatorial explosion, to practically an infinite number of molecular forms. This process is particularly valid on passing to the nanocosmos size category. The nanocosmos as such does not show the variety-limiting translational symmetry restriction of macroscopic crystalline materials but offers — unlike the microcosmos with its small molecules — the possibility of existence of larger arrays with local symmetries which are not in agreement with the overall symmetry. This is a well-known situation for spherical viruses with their hexagonal arrays. Figure 6 shows a model of the protein subunits of the Tomato Bushy Stunt Virus (TBSV) as an icosadeltahedron.[41,42]

In order to get a huge variety of structures the appropriate fragments chosen as building blocks should display a certain type of flexibility, which is a prerequisite for an extreme linking versatility of course not reaching by far that of amino acids.¶ This condition is well fulfilled by molybdenum-oxide based fragments which are collected as (virtual) building units in a 'dynamic library' with a potential to participate in a sort of 'split and link' processes depending on slight alterations of the relevant boundary conditions.

Remarkable in this context is the synthesis of a rather unusual giant molybdenum-oxide based nanocluster with the size of hemoglobin containing 368 metal and 1880 non-hydrogen atoms. The cluster has been formed by linking 64 $\{Mo_1\}$-, 32 $\{Mo_2\}$- and 40 $\{Mo(Mo_5)\}$-type units. The formation process was accompanied by a remarkable symmetry breaking process, which is nicely recognisable at the cluster surface. The preparation of the $\{Mo_{368}\}$ nanocluster can be considered as the starting point for the synthesis of quite a number of other clusters with a comparable or even larger size. Referring to the present discovery we would like to attract attention to the momentous and far-reaching step into the nanocosmos with perspectives for nanochemistry (*via* symmetry breaking), molecular topology and surface sciences with catalytical relevance. The above-mentioned symmetry breaking can be considered in relation to a transition from positive to negative surface areas, *i.e.*, the monotony breakdown.

¶ This special situation of versatility could lead us, using a term from J-M Lehn's lectures, to the category '*Multiple Expression of Molecular Information*', a statement which can be related to the formation of the variety of giant clusters obtained from relevant substance 'libraries'.

2. Synthesis and structure

The reduction of a molybdate solution acidified by sulfuric acid gives the dark blue compound [17]

$$Na_{48}[H_xMo_{368}O_{1032}(H_2O)_{240}(SO_4)_{48}]\cdot ca.\ 1000\,H_2O\ ,$$

6

which contains the giant mixed-valence cluster anion **6a** (Fig. 7).

$$[H_x\{Mo(Mo_5)\}'_8\{Mo(Mo_5)\}''_{32}\{Mo_2\}'_{16}\{Mo_2\}''_8\{Mo_2\}'''_8\{Mo_1\}_{64}]^{48-},$$

6a

with $\{Mo(Mo_5)\}' \equiv \{Mo_6O_{21}(H_2O)_6\}$; $\{Mo(Mo_5)\}'' \equiv \{Mo_6O_{21}.(H_2O)_3(SO_4)\}$; $\{Mo_2\}' \equiv \{Mo_2O_3(H_2O)_2\}$; $\{Mo_2\}'' \equiv \{Mo_2(O_t)_2.(O_{br})_3(SO_4)\}$; $\{Mo_2\}''' \equiv \{Mo_2(O_t)_4(O_{br})(SO_4)\}$; $\{Mo_1\} \equiv \{MoO(H_2O)\}$; $x \approx 16$.

Compound **6** crystallises in the space group *I*4*mm*, its unit cell comprises two giant blue lemon-like cluster anions **6a** with approximate D_4 symmetry; the anion has a nearly spherical $\{Mo_{288}O_{784}(H_2O)_{192}(SO_4)_{32}\}$ central fragment (**B**) and two $\{Mo_{40}O_{124}(H_2O)_{24}(SO_4)_8\}$ capping areas (**C**). As the average degree of reduction of the caps **C** is lower than the central fragment **B,** it is reasonable to suggest that the pathway to anion **6a** includes the initial formation of a fragment that resembles in shape the central fragment (**B**) of **6a** while owing to its more nucleophilic nature, it in turn gets capped by two more electrophilic caps **C** in course of the growth process (this refers to a relative consideration). The fragments **B** and **C** have local symmetries (see Fig. 7 *a*), D_{8d} and C_{4v}, respectively. Figure 7 *a* shows a clearly well-defined cross-section where the symmetry breaking [43–45] occurs and a negative curvature is generated. It should be noted that the linking of fragments **B** and **C**, characterised by different local symmetry, occurs through vertices rather than edges of the corresponding polyhedra. This was to be expected, as this pattern ensures a higher flexibility.

More precisely, the anion **6a** is built up by the six well-defined building units mentioned above, namely, $\{Mo(Mo_5)\}'$, $\{Mo(Mo_5)\}''$, $\{Mo_2\}'$, $\{Mo_2\}''$, $\{Mo_2\}'''$ and $\{Mo_1\}$ (see Fig. 7 *a*), which are linked to produce the giant molecular container (vase) of **6a** with a giant cavity (diameter $d \approx 2.5 \times 4.0$ nm at the most extended points). This cavity can accommodate an enormous number ($\sim$400) of water molecules. Of the 1000 (crystal) water molecules indicated in the formula of **6**, 400 molecules are encapsulated inside the cavity.

The presence of the bidentate SO_4^{2-} ligands is indicated in the vibrational spectrum by a typical splitting of the $\nu_3(F_2)$-type vibrational bands (1191, 1122 and 1060 cm^{-1}), while the presence of Mo^V centres along with the Mo^{VI} centres causes the IVCT (intervalence charge transfer) band at $\sim$740 nm. As can be seen from the above formula, the anion **6a** incorporates two types of $\{Mo(Mo_5)\}$ building units differing in the type of ligands. Thirty two $\{Mo(Mo_5)\}''$ blocks containing SO_4^{2-} ions are present in fragments **B** and eight $\{Mo(Mo_5)\}'$ blocks which do not contain these ligands are located in the caps **C**. The binuclear $\{Mo_2\}$ building units differ not only by the type of ligands but also by the type of coordination. Thus both Mo atoms of the $\{Mo_2\}'''$ fragments located at the ends of both caps **C** contain two terminal oxygen atoms. This situation seems to be characteristic of growth termination. The $\{Mo_1\}$ units are of the classical type, $\{OMo^V(H_2O)\}^{3+}$; they contribute significantly to the highly reduced state of anion **6a** (64 of the 112 Mo^V atoms belong to these fragments). The remaining 48 Mo^V-type centres are formally



Figure 6. Drawing of an icosadeltahedron ($T = 3$) as a model for the topologically identical protein coat subunits of the Tomato Bushy Stunt Virus (TBSV). The drawing was taken from Ref. 41. The orange lobes are packed about the icosadeltahedron fivefold axes, whereas the blue and green lobes alternate about its local sixfold axes, not allowed for an icosahedral symmetry group.

distributed over several parts of the cluster areas which causes a widespread delocalisation of Mo(4*d*) electrons.

The structure of **6a** can be considered as a hybrid between the giant ring-shaped cluster of the $\{Mo_{176}\}$ type [5–7] and the spherical $\{Mo_{102}\}$-type cluster.[36] In the cluster **6a**, one can find both: the $\{Mo(Mo_5)\}$ and $\{Mo_1\}$ fragments, typical for the spherical $\{Mo_{102}\}$ cluster, as well as the $\{Mo(Mo_5)\}$ and $\{Mo_2\}$ fragments, typical for ring-shaped systems. The hybrid character of cluster **6a** also becomes obvious due to the presence of 24 $\{Mo_{11}\}$ groups with C_5 symmetry and 16 $\{Mo_{10}\}$ groups with C_s symmetry, containing one MoO_6 octahedron less (Fig. 8).[7] (Note that the two groups have 56 MoO_6 octahedra in common; see Fig. 7 *a*.) The $\{Mo_{11}\}$ groups with C_5 symmetry are identical to those of the spherical clusters,[7] and the $\{Mo_{10}\}$ groups are identical to the $\{Mo_{10}\}$ fragment encountered in ring-shaped clusters, *i.e.* the $\{Mo_{11}\}$ group without the displaced MoO_6 octahedron.†

† The spherical- ($n = 12$) and ring-type ($n = 14, 16$) cluster species can be expressed by the same basic type of stoichiometry $\{Mo_{11}\}_n$, *i.e.*, they differ only in numbers n; this was categorised by us as a Pythagorean harmony.[7]

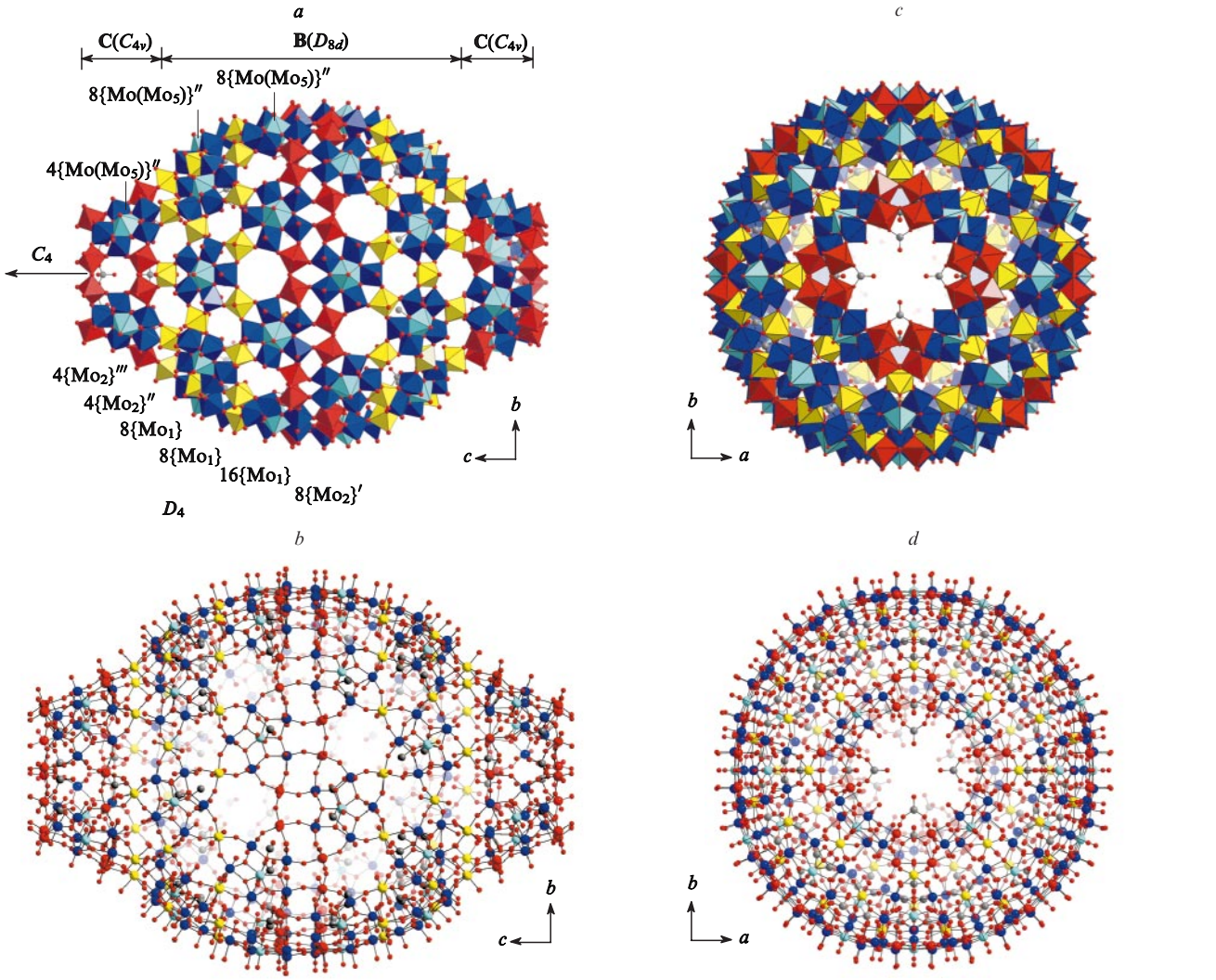


Figure 7. Structure of **6a** in crystals of **6** in polyhedral (*a*, *c*) and atomic (*b*, *d*) representations perpendicular to the C_4 axis (*a*, *b*) and along the C_4 axis (*c*, *d*). Building units: $\{Mo_1\}$, yellow; $\{Mo_2\}$, red; $\{Mo(Mo_5)\}$, blue with blue-turquoise pentagonal bipyramids; the O atoms are small red spheres, the S atoms are grey spheres. Note that one capping part is turned against the other by 360/16°. Different building blocks and the arrays of different local symmetry are marked. This drawing was first published in Ref. 17.

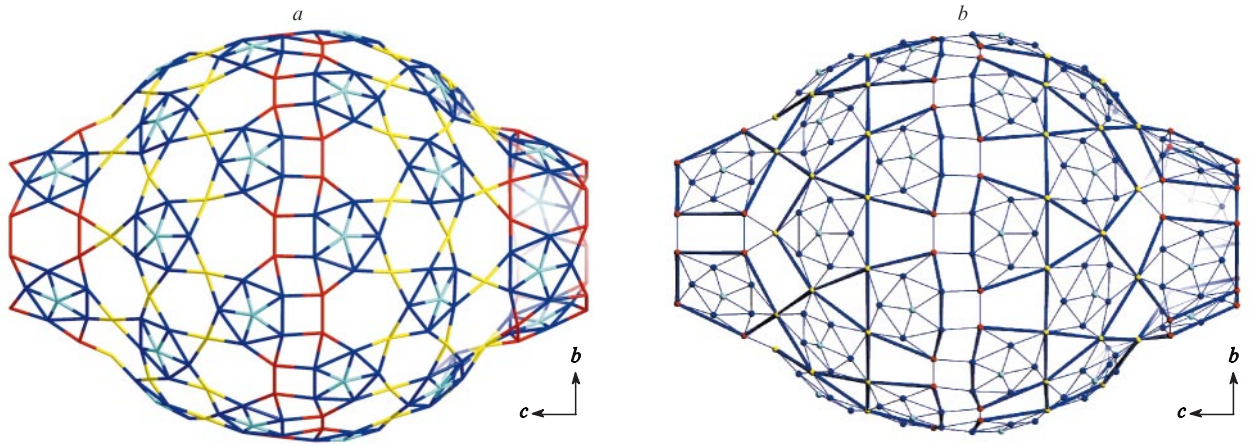


Figure 8. $\{Mo_{368}\}$ metal atom framework of **6a** in wire-frame (*a*) and atomic (*b*) representations. For colour designations, see Fig. 7*a*. The $\{Mo_{11}\}$ and $\{Mo_{10}\}$ building blocks in (*b*) are emphasised through thick lines.

The high degree of reduction (about 112 Mo^{V} and 256 Mo^{VI}) of **6a**, which is much higher than that in the ring systems (for example, 28 $Mo^{V}$and 126 Mo^{VI})[5] indicates that the cluster growth is promoted by reducing conditions. The largest cluster obtainable in an acidified molybdate solution in the absence of a reducing agent is the rather small $\{Mo_{36}\}$ anion,‡ which, however, 'starts growing' upon the addition of a reducing agent.[5] It is also significant that the higher the negative charge of the anion, the less probable is its uncontrolled linking but it initiates further protonation, which is a prerequisite for further linking. The high negative charge of anion **6a** is also influenced by the presence of SO_4^{2-} ligands coordinated to the intermediates and to the final cluster species. When the reaction is performed in the presence of the weakly coordinating ligands such as Cl^- or ClO_4^- (which do not appear in the cluster when $HClO_4$ or HCl are used as acidification agents, instead of H_2SO_4), the reaction affords only ring-like molybdenum-oxide based species[5] rather than the hybrid cluster **6a**. It is also worth mentioning that, although the coordination capacity of SO_4^{2-} is higher than those of Cl^- or ClO_4^-, it is still not too strong; thus, it provides a coordination flexibility and, as a consequence, generation of a variety of different appropriate building blocks. The average degree of reduction of the two $\{Mo_{40}\}$-type caps (**C**) in cluster **6a** is lower than that of the central fragment **B**. This observation agrees with our hypothesis that growth processes in polyoxometallate-type systems are mostly based on nucleophiles which form the initial fragment of the cluster and direct the formation of electrophiles by which they get capped (electrophiles and nucleophiles in a relative consideration).

As examples of such growth, one can consider the transition from a hypothetical extremely negatively charged V^{IV}-type Keggin ion to the stable cluster formed upon capping the Keggin ion with six additional VO^{2+} groups;[1,2,47] the transition from the $\{Mo_{57}\}$-type cluster to the extended $\{Mo_{63}\}$ cluster (*via* linking of $\{Mo_{57}\}$ to six MoO^{4+} groups[48]); and the transition from the $\{Mo_{176}\}$-type cluster anion to the $\{Mo_{248}\}$ anion *via* linking of $\{Mo_{176}\}$ to two neutral $\{Mo_{36}\}$ fragments.[49] A further example refers to remarkable processes occurring during the formation of the unusual unsymmetrical molybdenum-oxide based $\{Mo_{37}\}$ cluster. After a highly reduced ε-Keggin-type $\{Mo^{V}_{12}\}$ unit is capped by four electrophilic $\{MoO_3\}$ groups, these groups get reduced while the resulting $\{Mo_{16}\}$ species is capped by the positively charged $\{Mo_{11}\}$ and $\{Mo_{10}\}$ fragments. Often, processes of this type result in a lowering of the unusually high negative charge of the intermediates. In each of the examples described above, the central nucleophilic core appears to have directed the formation of electrophilic fragments.

3. Perspectives

The knowledge of structural details of cluster **6a** will probably be the starting point for the synthesis of many other systems of comparable sizes as well as for the development of a new type of nanochemistry characterised by performing well-defined reactions at specified sites of well-defined nanoobjects and also includes their handling as intact units for instance for the preparation of composites, *e.g.*, with silica and additionally surfactants to give micelles, films, and even liquid crystals.[10–14,50,51] (The possibility of these studies is indicated by the syntheses and use of the giant spherical and ring clusters mentioned above.) The present results with the cluster having a giant surface also seem to be of relevance for some aspects of catalysis, as it is still a challenge to understand the details of the interaction mechanisms of substrates with the surfaces of heterogeneous catalysts.[52–55] In the case of transition metal oxides, like MoO_3, which play an important role in selective oxidation processes,[54,55] it would be a tremendous step forward to consider the surfaces of discrete and well-defined giant molybdenum-oxide based clusters for modelling catalytic reactions [note that the large surface of **6a** contains only Mo = O and $Mo(H_2O)$ groups].§ This would help to understand the surface properties for related catalytically active bulk materials which are difficult to investigate.[56]

Another interesting aspect is the possibility of performing reactions within the cavity of the giant molecular container **6a**, the largest structurally well-defined one known, while for instance encapsulation-type reactions resulting in a novel type of supramolecular compounds are known for even smaller spherical clusters.[28,57] This type of nanochemistry/nanotechnology and supramolecular engineering[58,59] is based on the use of thoroughly characterised objects obtained by the 'bottom-up' method.

Symmetry breaking,[43–45] observed in many natural processes, can be modelled by the present reaction. The symmetry breaking occurs here due to the presence of different local symmetry areas on the surface of **6a** as in the case of Fowler's Phantasmagorical Fulleroids, due to the presence of negative and positive curvatures. Symmetry breaking is also relevant for the understanding of patternings in the macrocosmos including those cases where the antagonistic effects are important.[60–65] This phenomenon was described long ago by D'Arcy Thompson in his famous book '*On Growth and Form*'.[62] A remarkable example of symmetry breaking

‡ When the paper[46] dealing with the structure of $\{Mo_{36}\}$ was published, it was considered to be the largest inorganic anion(!).

§ The presence of the large number of $\{O=MoO_6\}$-type pentagonal bipyramids in **6a** is interesting as this group is considered to be responsible for important types of selective oxidations based on molybdenum oxide catalysts.[53]

was discussed by L Addadi and S Weiner.[66] They considered the formation of asymmetrical shapes during the growth of crystalline structures. The authors refer in this context to the famous Curie symmetry principle [67] (see also Refs 68, 69), which, as the authors state, cannot be generalised. It is also not fulfilled in our particular case, *i.e.*, when fragment **B** is regarded as inducing the 'growth' of the other fragment **C**. Addadi and Weiner [66] consider the above-mentioned process to be the first step towards understanding asymmetry in biology.

It would be a breakthrough if rather large nanoareas, such as **B** and **C** with different symmetries, could be further extended. In particular, this should be of course more easily possible under dissipative conditions.

The formation of **6a** under conservative conditions shows a type of patterning, emergence, and complexity at a nanolevel, not as is mostly considered at a macrolevel case, as, for instance, in the situations of dissipative self-organisation model processes leading to Bénard convection cells and to Belousov–Zhabotinsky-type reactions.[61] The novelty of the present nanoobject is that symmetry breaking is observed during growth, *i.e.* self-assembly. This is caused by different distributions of a rather large number of different negative and positive vertices with polygons ranging from triangles to heptagons (Fig. 9). The complexity of the structure of cluster **6a** can be demonstrated by comparison with the Archimedean solids having only one type of vertex.

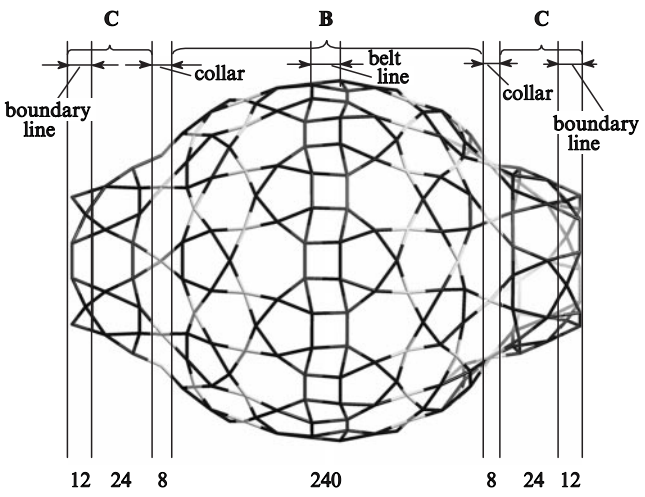


Figure 9. The four regular polyhedron depicting the surface of **6a**, consisting of 328 = 368−40 Mo atoms (*i.e.*, without the Mo atoms of the pentagonal bipyramids). The polyhedron has 240 vertices in the central fragment **B**. 64 vertices are in the belt region, 32 vertices with the vertex configuration [3,4,4,5], 32 of the type [3,4,4,7]; 16+8 of the type [3,5,3,7], 8 of the type [3,5,3,6], and 16 of the type [3,6,3,7] are in each of the two B regions next to the belt and another two times 16, 8, and 16 with a vertex configuration of the type [3,5,3,6], [3,6,3,7], and [3,5,3,7], respectively, are next to the two collars, altogether 16 of type [3,7,3,7] along the two collars, 8 of types [3,6,3,7], [3,5,3,7], and [3,5,3,6] each in the interior of the two capping regions, and 4 of type [3,5,3] and 8 of type [3,6] along each of the two boundary lines. This drawing was first published in Ref. 17.

4. Combinatorial topology of the polyhedral structure of nanoclusters: relevance for the present symmetry breaking processes

This Section explains first of all the topological nature of the surface of **6a** but it could also be useful for a chemist in constructing rather large patterns showing positive and negative curvatures. Combinatorial analysis of the four regular polyhedral net formed by the Mo atoms in **6a**, as shown in Fig. 9 (for simplicity, the Mo atoms within the interior of the pentagonal bipyramids are omitted), reveals a clear correspondence between the overall distribution of positively and negatively curved surface segments (for illustration, examples of positively and negatively curved surfaces are given, Fig. 10) and the distribution of vertices with positive and negative combinatorial curvature. This is in line with the well-known Euler's theorem,[70] interpreted as a discrete version of the Gauss–Bonnet theorem.

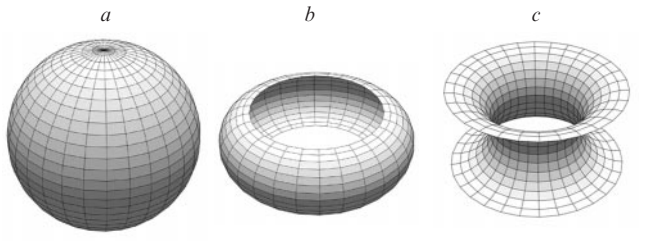


Figure 10. Shapes of positively (*a*, *b*) and negatively (*c*) curved surfaces. The sphere and the outer part of a torus are paradigms of surfaces exhibiting positive curvature (*a*, *b*); the saddle and the inner part of a torus are paradigms of surfaces exhibiting negative curvature (*c*).

Indeed, the surfaces of the central fragment **B** with D_{8d} symmetry and two capping regions **C** with C_{4v} symmetry are positively curved. The fragments **B** and **C** are connected by the two narrow collars exhibiting a strong indentation, thus creating two ring-shaped surface components of large negative curvature of relevance for the symmetry breaking. Additional negative curvature is 'hidden' in the jaggedness of the two circular boundary lines (see Fig. 9). Indeed, straightening them out into circles would create shapes that would each mimic the shape of a neck, *i.e.*, one half of the negatively curved inner part of a torus (see Fig. 10). The important role of pentagons and heptagons in the case of Fowler's Phantasmagorical Fulleroids is clearly illustrated by Fig. 11. Any fulleroid with icosahedral symmetry consisting of only pentagons and heptagons contains exactly $12+60N$ pentagons and $60N$ heptagons for some positive integer N. There are two such fulleroids with $N=1$. In one of them, 72 pentagons are grouped in 12 sets each containing 6 pentagons. Each set generates the outcrops of a high positive curvature counterbalanced by a network of negatively curved channels built from its 60 heptagons, which results in a net positive curvature of four as required. The other one consists of 12 separate pentagons and 20 sets of three pentagons each, which are also connected by a network of negatively curved channels built from the heptagons exhibiting, however, a much smoother geometry because of the much better local balance of positive and negative curvature. Figure 11 shows the structures of two Fowler's Phantasmagorical Fulleroids, illustrating how areas

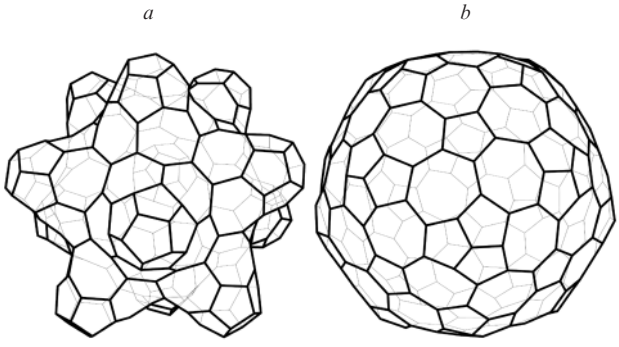


Figure 11. Fowler's Phantasmagorical Fulleroid structures (see Ref. 17 with related references).

exhibiting strongly positive curvature can be intertwined with areas exhibiting negative curvature to produce a surface of only moderately positive curvature.

V. Conclusion

The use of the cluster building blocks present in solutions of polyoxometallates and linking of special fragments such as the pentagonal-type {Mo(Mo$_5$)} units by different types of linkers, *e.g.* paramagnetic (open shell) centres opens up new fascinating perspectives for nano-, supramolecular, solid-state and magneto-chemistry. 'Playing' with pentagons not only can result in several giant spherical, quasi-spherical and circular species, but it is also of interest because of their role in the history of culture, virology, the geodesic domes of Fuller, and certain aspects of solid-state physics (see the fascinating quasicrystals). A special challenge will be, for instance, to fill the cavities and pores of nanoobjects such as of the spherical {Mo$_{132}$} cluster with a variety of different guests and also to place molecules inside the cavities of ring-shaped clusters, resulting in different reactivities compared to those of the discrete (isolated nano-sized) ones.

We believe that the title of this review is justified, as our topic allows an unusual type of nanochemistry by performing controlled reactions at well-defined sites of structurally well-defined nanoobjects. Since such nanoobjects can be used as building blocks for the construction of extended structures based on crystal engineering, this field opens up new perspectives for solid-state chemistry, which becomes defined and accurate even up to the atomic level. It has been a long and thorny but successful way in polyoxometallate chemistry since 1956, when Jonassen and Kirschner published a review referring to the knowledge of that time and to the major earlier contributions of important chemists like Rosenheim, Werner, Pfeiffer, Pauling and Keggin.[71]

We thank Prof. M Luban, Dr. P Kögerler (Ames Laboratories, Iowa State University, USA) and Dr. H Bögge (Bielefeld University, Germany) for their collaboration. The financial support of the German Research Society (Deutsche Forschungsgemeinschaft), the Foundation for Chemical Industry (Fonds der Chemischen Industrie), and the European Commission is gratefully acknowledged. S Roy thanks the Graduiertenkolleg 'Strukturbildungsprozesse', Bielefeld University, for a fellowship.

References

1. M T Pope, A Müller *Angew. Chem., Int. Ed. Engl.* **30** 34 (1991)
2. A Müller, H Reuter, S Dillinger *Angew. Chem., Int. Ed. Engl.* **34** 2328 (1995)
3. A Müller, F Peters, M T Pope, D Gatteschi *Chem. Rev.* **98** 239 (1998)
4. A Müller, P Kögerler, C Kuhlmann *Chem. Commun.* 1347 (1999)
5. A Müller, C Serain *Acc. Chem. Res.* **33** 2 (2000)
6. L Cronin, P Kögerler, A Müller *J. Solid State Chem.* **152** 57 (2000)
7. A Müller, P Kögerler, H Bögge *Struct. Bonding* (*Berlin*) **96** 203 (2000)
8. A Müller, P Kögerler, A Dress *Coord. Chem. Rev.* **222** 193 (2001)
9. O Delgado, A Dress, A Müller, in *Polyoxometalate Chemistry: From Topology via Self-Assembly to Applications* (Eds M T Pope, A Müller) (Dordrecht: Kluwer Academic, 2001) p. 69
10. D G Kurth, P Lehmann, D Volkmer, H Cölfen, M J Koop, A Müller, A Du Chesne *Chem. Eur. J.* **6** 385 (2000)
11. D Volkmer, A Du Chesne, D G Kurth, H Schnablegger, P Lehmann, M J Koop, A Müller *J. Am. Chem. Soc.* **122** 1995 (2000)
12. D G Kurth, D Volkmer, M Ruttorf, B Richter, A Müller *Chem. Mater.* **12** 2829 (2000)
13. D G Kurth, P Lehmann, D Volkmer, A Müller, D Schwahn *J. Chem. Soc., Dalton Trans.* 3989 (2000)
14. F Caruso, D G Kurth, D Volkmer, M J Koop, A Müller *Langmuir* **14** 3462 (1998)
15. A Müller, E Krickemeyer, H Bögge, M Schmidtmann, P Kögerler, C Rosu, E Beckmann *Angew. Chem., Int. Ed.* **40** 4034 (2001)
16. A Müller, S K Das, M O Talismanova, H Bögge, P Kögerler, M Schmidtmann, S S Talismanov, M Luban, E Krickemeyer *Angew. Chem., Int. Ed.* **41** 579 (2002)
17. A Müller, E Beckmann, H Bögge, M Schmidtmann, A Dress *Angew. Chem., Int. Ed.* **41** 1162 (2002)
18. A Müller, E Krickemeyer, H Bögge, M Schmidtmann, F Peters *Angew. Chem., Int. Ed.* **37** 3360 (1998)
19. A Müller, E Krickemeyer, J Meyer, H Bögge, F Peters, W Plass, E Diemann, S Dillinger, F Nonnenbruch, M Randerath, C Menke *Angew. Chem., Int. Ed. Engl.* **34** 2122 (1995)
20. A Müller, S K Das, E Krickemeyer, C Kuhlmann *Inorganic Syntheses* Vol. 34 (Ed. J Shapley) (New York: Wiley, in the press)
21. J-M Lehn, in *Chemistry for the 21st Century* (Eds E Keinan, I Schechter) (Weinheim: Wiley-VCH, 2001) p. 1
22. J Rosen, in *Symmetry in Science: An Introduction to the General Theory* (New York: Springer, 1995)
23. H Genz *Symmetrie: Bauplan der Natur* (München: Piper, 1987)
24. A Müller, S K Das, H Bögge, M Schmidtmann, A Botar, A Patrut *Chem. Commun.* 657 (2001)
25. A Müller, S K Das, C Kuhlmann, H Bögge, M Schmidtmann, E Diemann, E Krickemeyer, J Hormes, H Modrow, M Schindler *Chem. Commun.* 655 (2001)
26. A Bielanski, A Malecka-Lubanska, J Pozniczek, A Müller, E Krickemeyer, E Diemann *Bull. Pol. Acad. Sci., Chem.* **49** 85 (2001)
27. A K Cheetham, G Firey, T Loiseau *Angew. Chem., Int. Ed.* **38** 3268 (1999)
28. A Müller, S K Das, P Kögerler, H Bögge, M Schmidtmann, A X Trautwein, V Schmnemann, E Krickemeyer, W Preetz *Angew. Chem., Int. Ed.* **39** 3413 (2000)
29. A V Soldatov, G Roth, A Dzyabchenko, D Johnels, S Lebedkin, C Meingast, B Sundqvist, M Haluska, H Kuzmany *Science* **293** 680 (2001)
30. H Brumm, E Peters, M Jansen *Angew. Chem., Int. Ed.* **40** 2069 (2001)
31. G-W Wang, K Komatsu, Y Murato, M Shiro *Nature (London)* **387** 583 (1997)
32. C Schlenker (Ed.) *Low Dimensional Electronic Properties of Molybdenum Bronzes and Oxides* (Dordrecht: Kluwer Academic, 1984)
33. A Müller, S Sarkar, S Q N Shah, H Bögge, M Schmidtmann, Sh Sarkar, P Kögerler, B Hauptfleisch, A X Trautwein, V Schünemann *Angew. Chem., Int. Ed.* **38** 3238 (1999)
34. A Müller, S K Das, E Krickemeyer, P Kögerler, H Bögge, M Schmidtmann *Solid State Sci.* **2** 847 (2000)
35. A Müller, M Luban, C Schröder, R Modler, P Kögerler, M Axenovich, J Schnack, P Canfield, S Budko, N Harrison *ChemPhysChem* **2** 517 (2001)
36. A Müller, S Q N Shah, H Bögge, M Schmidtmann, P Kögerler, B Hauptfleisch, S Leiding, K Wittler *Angew. Chem., Int. Ed.* **39** 1614 (2000)
37. N W Ashcroft, N D Mernin *Solid State Physics* (Philadelphia: Saunders College, 1976)
38. J B Goodenough, in *Chemical Uses of Molybdenum* (*Proceedings of the 4th International Conference on Molybdenum*) (Eds H F Barry, P C H Mitchel) CLIMAX Molybdenum Co., MI, 1982, p. 1
39. S A Borshch, H Duclusaud, in *Polyoxometalate Chemistry: From Topology via Self-Assembly to Applications* (Eds M T Pope, A Müller) (Dordrecht: Kluwer Academic, 2001) p. 135
40. H So, M T Pope, in *Electron and Proton Transfer in Chemistry and Biology* (Eds A Müller, H Ratajczak, W Junge, E Diemann) (Amsterdam: Elsevier, 1992) p. 71
41. D Voet, J G Voet, in *Biochemistry* (2nd Edition) (New York: Wiley, 1995) p. 1082
42. A Müller, E Beckmann, H Bögge, M Schmidtmann, A Dress *Angew. Chem., Int. Ed.* **41** 1162 (2002)
43. H Genz *Symmetrie und Symmetriebrechung in der Physik* (Braunschweig: Vieweg, 1991)
44. H Haken *Synergetics* (3rd Edition) (Berlin: Springer, 1983)
45. K Mainzer *Thinking in Complexity* (3rd Edition) (Berlin: Springer, 1997)
46. K-H Tytko, B Schönfeld, B Buss, O Glemser *Angew. Chem., Int. Ed. Engl.* **12** 330 (1973)

47. A Müller, R Sessoli, E Krickemeyer, H Bögge, J Meyer, D Gatteschi, L Pardi, J Westphal, K Hovemeier, R Rohlfing, J Döring, F Hellweg, C Beugholt, M Schmidtmann *Inorg. Chem.* **36** 5239 (1997)
48. A Müller, J Meyer, E Krickemeyer, C Beugholt, H Bögge, F Peters, M Schmidtmann, P Kögerler, M J Koop *Chem. Eur. J.* **4** 1000 (1998)
49. A Müller, S Q N Shah, H Bögge, M Schmidtmann *Nature* (*London*) **397** 48 (1999)
50. S Polarz, B Smarsly, C Göltner, M Antonietti *Adv. Mater.* **12** 1503 (2000)
51. S Polarz, B Smarsly, M Antonietti *ChemPhysChem.* **2** 457 (2001)
52. A Müller, R Maiti, M Schmidtmann, H Bögge, S K Das, W Zhang *Chem. Commun.* 2126 (2001)
53. G Mestl, C Linsmeier, R Gottschall, M Dieterle, J Find, D Herein J Jäger, Y Uchida, R Schlögl *J. Mol. Catal. A: Chem.* **162** 455 (2000)
54. J Haber, L Lalik *Catal. Today* **33**C 119 (1997)
55. J Haber, in *Molecular Mechanism of Heterogeneous Oxidation — Organic and Solid State Chemists Views in Studies in Surface Science and Catalysis* Vol. 110 (Eds B Delmon, Y T Yates) (Amsterdam: Elsevier, 1997) p. 1
56. V E Henrich, P A Cox *The Surface Science of Metal Oxides* (Cambridge: Cambridge University Press, 1994)
57. S Hurtley (Ed.) *Editor's Choice, Highlights of the Recent Literature. Science* **290** 411 (2000)
58. B C Crandall, J Lewis (Eds) *Nanotechnology: Research and Perspectives* (Cambridge: MIT Press, 1992)
59. J Simon, P Bassoul *Design of Molecular Materials: Supramolecular Engineering* (Chichester: Wiley, 2000)
60. E Ben-Jacobs, H Levine *Nature* (*London*) **409** 985 (2001)
61. H Haken, A Wunderlin *Die Selbststrukturierung der Materie: Synergetik in der unbelebten Welt* (Braunschweig: Vieweg, 1991)
62. D'Arcy Thompson *On Growth and Form* (Cambridge: Cambridge University Press, 1961) (Canto Edition, 1997)
63. A M Turing *Philos. Trans. R. Soc. London B* **237** 37 (1952)
64. K Mainzer, A Müller, W G Saltzer (Eds) *From Simplicity to Complexity, Part II: Information–Interaction–Emergence* (Braunschweig: Vieweg, 1998)
65. P Ball *The Self-Made Tapestry: Pattern Formation in Nature* (Oxford: Oxford University Press, 1999)
66. L Addadi, S Weiner *Nature (London)* **411** 753 (2001)
67. P Curie *J. Phys.* (*Paris*) **3** 393 (1894)
68. I Hargittai, M Hargittai, in *Our Own Image: Personal Symmetry in Discovery* (New York: Kluwer Academic, 2000) p. 216
69. I Hargittai, M Hargittai *Symmetry through the Eyes of a Chemist* (Weinheim: VCH, 1986)
70. H S M Coxeter, in *Introduction to Geometry* (New York: Wiley, 1989) p. 152
71. H B Jonassen, S Kirschner, in *The Chemistry of the Coordination Compounds* (Eds J C Bailar Jr, D H Busch) (New York: Reinnhold, 1956)